

A discontinuous transition from direct to inverse cascade in three-dimensional turbulence

Ganapati Sahoo¹, Alexandros Alexakis² and Luca Biferale¹

¹ *Department of Physics and INFN, University of Rome 'Tor Vergata',
Via della Ricerca Scientifica 1, 00133 Rome, Italy. and*

² *Laboratoire de Physique Statistique, École Normale Supérieure, CNRS,
Université Pierre et Marié Curie, Université Paris Diderot, 24 rue Lhomond, 75005 Paris, France.*

Inviscid invariants of flow equations are crucial in determining the direction of the turbulent energy cascade. In this work we investigate a variant of the three dimensional Navier-Stokes equations that shares exactly the same ideal invariants (energy and helicity) and the same symmetries (under rotations, reflexions and scale transforms) as the original equations. It is demonstrated that the examined system displays a change in the direction of the energy cascade when varying the value of a free parameter which controls the relative weights of the triadic interactions between different helical Fourier modes. The transition from a forward to inverse cascade is shown to occur at a critical point in a discontinuous manner with diverging fluctuations close to criticality. Our work thus supports the observation that purely isotropic and three dimensional flow configurations can support inverse energy transfer when interactions are altered and that inside all turbulent flows there is a competition among forward and backward transfer mechanism which might lead to multiple energy-containing turbulent states.

In turbulent systems the direction of the energy cascade determines the macroscopic properties of the flow leading to a finite energy dissipation rate in the case of a forward cascade (from large to small scales) or to the formation of a condensate in the case of an inverse cascade (from small to large scales) [1]. It has been long thought that the direction of cascade is determined by the dimensionality and the ideal invariants of the flow. Two dimensional (2D) turbulence possesses two sign definite invariants, the energy and the enstrophy. Energy is transferred backward to larger scales while enstrophy is transferred forward to the small scales. On the other hand, in three dimensional (3D) turbulence while energy is sign definite, the second invariant, the helicity, is sign indefinite. As a result, helicity does not put any local or global constraints on the direction of the energy transfer and it is an empirical fact that in 3D turbulent flows both energy and helicity are transferred to small scales [2, 3].

There are systems which develop a more complex phenomenology, e.g. flows in thin layers, in a stratified medium, in the presence of rotation or of magnetic field show a quasi-2D behavior [4–13] and display a bidirectional split energy cascade: part of the energy goes towards small scales (as in 3D) and part to the large scales (as in pure 2D flows). This phenomenon has been observed also in recent experiments [14–16] and in atmospheric measurements [17]. The reason for the appearance of an inverse energy flux is ascribed to the presence of (resonant) waves or of geometric confinement, that favor the enhancement of quasi-2D Fourier interactions over the 3D background.

In this work we study a model system for which the interactions in the Navier-Stokes equations (NSE) are enhanced or suppressed in a controlled way without reducing the number of degrees of freedom, altering the invis-

cid invariants or breaking any of the symmetries of the NSE. Our study is based on the helical decomposition [18–21] of the velocity field \mathbf{u} , that in terms of its Fourier modes $\tilde{\mathbf{u}}_{\mathbf{k}}$ it is written as: $\tilde{\mathbf{u}}_{\mathbf{k}} = \tilde{u}_{\mathbf{k}}^+ \mathbf{h}_{\mathbf{k}}^+ + \tilde{u}_{\mathbf{k}}^- \mathbf{h}_{\mathbf{k}}^-$ where $\mathbf{h}_{\mathbf{k}}^\pm$ are the eigenvectors of the curl operator $i\mathbf{k} \times \mathbf{h}_{\mathbf{k}}^\pm = \pm \mathbf{h}_{\mathbf{k}}^\pm$. In real space the velocity field is written as $\mathbf{u} = \mathbf{u}^+ + \mathbf{u}^-$ where \mathbf{u}^\pm is the velocity field whose Fourier transform is projected to the \mathbf{h}^\pm base. It is easy to realize that in terms of the helical decomposition the nonlinear term of the 3D NSE is split in 4 (8 by considering the obvious symmetry that changes the sign of all helical modes) possible classes of helical interactions, corresponding to triads of helical Fourier modes, $(\tilde{u}_{\mathbf{k}}^\pm, \tilde{u}_{\mathbf{q}}^\pm, \tilde{u}_{\mathbf{p}}^\pm)$ as depicted by the four triadic families in Fig. 1. In the set of sim-

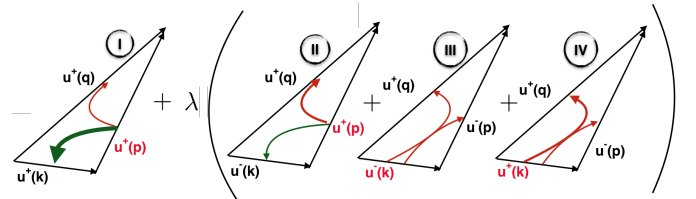


FIG. 1: (Color online) Sketch of the four classes of triadic interactions present in the exact helical-Fourier decomposition of NSE. Green (red) lines describe the backward (forward) energy transfer from the most unstable mode [21]. The thicker line corresponds to the dominant term.

ulations performed in this paper, we change the relative weight among homochiral triads (Class I) and all the others by introducing a factor $0 \leq \lambda \leq 1$ in the nonlinear evolution. We show that by using this weighting protocol the turbulent evolution displays a sharp transition, for a critical value λ_c , from forward to backward energy transfer but still keeping the dynamics fully three dimensional, isotropic and parity invariant. By analyzing the

dynamics of each class separately, it was shown in [21] that the homochiral triads (Class I in Fig. 1) always lead to an excess of energy transfer to large scales. On the other hand, the transfer direction of triads of Class-II depends on the geometry of the three interacting modes while Class III and IV always transfer energy forward. In [22, 23] it was shown that the above prediction is robust by demonstrating that if the NSE is restricted only to homochiral interactions (Class I) it displays a fully isotropic 3D inverse energy cascade. In [24], a system that transitioned from the NSE to that of homochiral triads[22, 23] was investigated by introducing a random decimation of modes with negative helicity with a varying probability, $0 \leq \alpha \leq 1$ ($\alpha = 0$ being the original NSE and $\alpha = 1$ being the system of homochiral triads). In that study, the transition from forward to inverse energy cascade happens in a quasi-singular way such that the inverse cascade exists only at $\alpha \sim 1$ demonstrating that even if only a small set of interactions among helical waves of both sign are present (Class II, III and IV), the energy transfer is always forward. Similar conclusions were reached by [25] where the amplitude of the negative helical modes was controlled by a dynamical forcing.

In this work we investigate a variant of the original NSE obtained by introducing different weighting of the 4 helical-Fourier classes, such as to smoothly interpolate from the full NSE to the reduced version where interactions among the \mathbf{u}^+ and the \mathbf{u}^- are forbidden of [22, 23], but without removing any modes. In particular, we evolve the following system:

$$\partial_t \mathbf{u} = \mathbb{P}[\mathcal{N}] - \nu \Delta^4 \mathbf{u} - \mu \Delta^{-2} \mathbf{u} + \mathbf{F} \quad (1)$$

where ν is the coefficient of the hyper-viscosity term and μ of the energy sink at large scale needed to arrest the inverse cascade of energy (if any). \mathbb{P} is a projection operator to incompressible fields. The nonlinearity \mathcal{N} is defined as:

$$\mathcal{N} = \lambda(\mathbf{u} \times \mathbf{w}) + (1-\lambda)[\mathbb{P}^+(\mathbf{u}^+ \times \mathbf{w}^+) + \mathbb{P}^-(\mathbf{u}^- \times \mathbf{w}^-)] \quad (2)$$

where $\mathbf{w} = \nabla \times \mathbf{u}$ is the vorticity, \mathbb{P}^\pm stands for the projection operator to the incompressible helical base with $\mathbf{u}^\pm = \mathbb{P}^\pm[\mathbf{u}]$ and $\mathbb{P} = \mathbb{P}^+ + \mathbb{P}^-$. This model, proposed in [26], is graphically summarized in Fig. 1. For any value of λ the inviscid system conserves the same quantities as the 3D NSE, namely the energy $E = \frac{1}{2} \langle \mathbf{u}^2 \rangle$ and the helicity $H = \frac{1}{2} \langle \mathbf{u} \cdot \mathbf{w} \rangle$ (where the angular brackets stand for spatial average) and has the same rotation, reflection and dilatation symmetries. For $\lambda = 1$, \mathcal{N} reduces to the nonlinearity of the NSE and energy cascades forward. For $\lambda = 0$ the two fields \mathbf{u}^\pm decouple and Eq.(1) becomes the equation examined in [22, 23]. It conserves two energies $E^\pm = \frac{1}{2} \langle (\mathbf{u}^\pm)^2 \rangle$ and two sign definite helicities $H^\pm = \frac{1}{2} \langle \mathbf{u}^\pm \cdot \mathbf{w}^\pm \rangle$ independently and cascades energy inversely. We thus expect that as λ is varied continuously from $\lambda = 1$ to $\lambda = 0$ there will be a change in the

Run	N	k_f	ν	μ	Re
N1K1	256	[10, 12]	10^{-14}	0.5	$6 \cdot 10^6$
N2K1	512	[10, 12]	10^{-16}	0.5	$6 \cdot 10^8$
N3K1	1024	[10, 12]	10^{-18}	0.5	$6 \cdot 10^{10}$
N2K2	512	[20, 22]	10^{-16}	0.5	$5 \cdot 10^6$

TABLE I: Parameters of the numerical simulations where $Re = \varepsilon_{inj}^{1/3} / (\nu k_f^{22/3})$. The large-scale friction proportional to μ was applied only for $k < k_\mu = 2$ in the simulations where we observe a inverse energy cascade.

direction of energy cascade from forward to inverse. The purpose of this work is to investigate how this transition takes place as the parameter λ is varied.

We perform a systematic series of high resolution numerical simulations of Eq. (1) in a box of size $L = 2\pi$ with spatial resolution of N^3 . Energy is injected at intermediate wavenumbers k_f by a Gaussian forcing delta correlated in time with a fixed injection rate ε_{inj} . We use a pseudo-spectral code, fully dealiased and with second order Adams-Bashforth time advancing scheme with exact integration of the viscous term. Table I lists the parameters for all simulations.

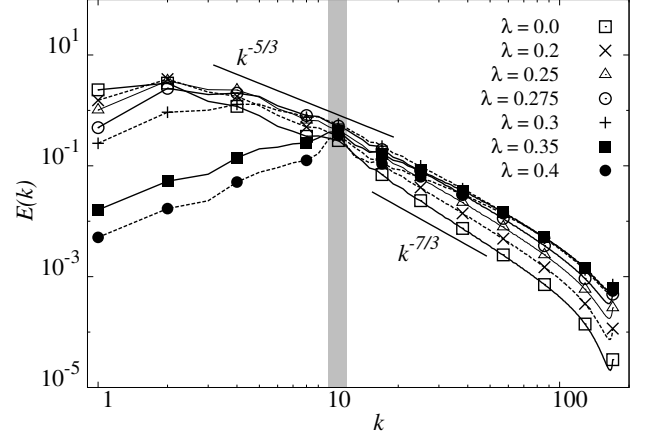


FIG. 2: (Color online) Log-log plot of energy spectra at changing λ and for fixed forcing range (runs N2K1 in Table I). The grey area denotes the forcing window. The two straight lines corresponds to the scaling predicted in presence an energy cascade and for the helicity cascade. Notice that for $\lambda > \lambda_c \sim 0.3$ there is no inverse energy cascade and the spectra agree well with $k^{-5/3}$ in the forward range. Contrary, for $\lambda < \lambda_c$ an inverse energy transfer develop and the forward scaling becomes closer to the one predicted for helicity transfer, i.e., $k^{-7/3}$.

Figure 2 shows the energy spectra measured at the steady state for different values of the parameter λ obtained from simulations N2K1. Clearly for large values of λ there is no significant energy in the large scales while small scales display a spectrum compatible with $k^{-5/3}$. For small values of λ , the energy is peaked at large scales forming a spectrum close to $k^{-5/3}$ while a steeper spec-

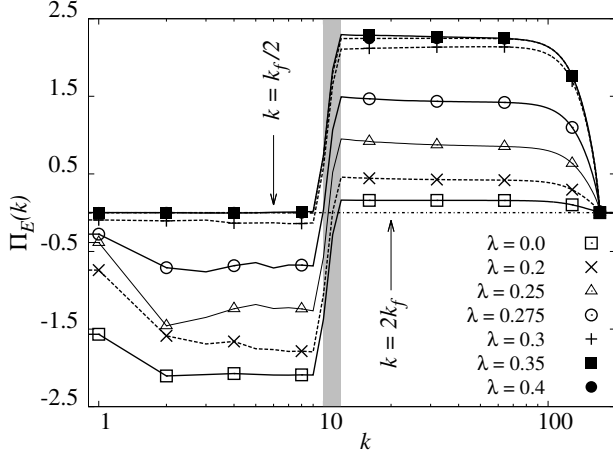


FIG. 3: Plots of energy flux for different values of λ . The gray band shows the forced range of wavenumbers. The arrows mark the wavenumbers at which we measure the fluctuations in the flux (see insets of Fig. 4).

trum closer to $k^{-7/3}$ is observed in the small scales. The two behaviors suggest a change from a forward to an inverse cascade, which is best demonstrated by looking at the energy fluxes depicted in Fig. 3. The energy flux is defined as

$$\Pi(k) = -\langle \mathbf{u}_k^< \cdot \mathcal{N} \rangle, \quad (3)$$

where $\mathbf{u}_k^<$ expresses the velocity field \mathbf{u} filtered so that its Fourier transform contains only wavenumbers \mathbf{k} satisfying $|\mathbf{k}| \leq k$, and expresses the rate energy is transferred out of the set of wavenumbers $|\mathbf{k}| \leq k$ to larger \mathbf{k} . $\Pi(k)$ is constant in the inertial ranges $k_\mu \ll k \ll k_f$ and $k_f \ll k \ll k_\nu$ (where $k_\mu \sim 1$ is the hypo-viscous wavenumber and $k_\nu \sim N/3$ the viscous-wavenumber). It is positive if the cascade is direct and negative if the cascade is inverse.

As λ is varied the direction of cascade is changing. For $\lambda \geq 0.3$ the flux is almost zero for $k < k_f$, while it is positive and constant for $k_f < k < k_\nu$. For $\lambda \leq 0.2$ the opposite picture holds. For $k < k_f$ the flux is negative and constant, while $k > k_f$ the flux is positive but weak. For values of λ in the range $0.2 < \lambda < 0.3$ we observe a bidirectional cascade: the co-existence of a forward and inverse transfer.

The bidirectional cascade is however a finite size effect and this behavior does not survive the large Reynolds and the large box-size (k_f) limit. This is demonstrated in Figure 4 where we examine how the inverse and forward fluxes change as the Reynolds number Re and the box size k_f are increased. The inverse flux (measured at the wavenumber $k = k_f/2$) as a function of λ for different values of the Reynolds numbers (grid-sizes) and different box sizes is shown in Fig. 4(a) while the forward energy flux (measured at the wavenumber $k = 2k_f$) is shown in Fig. 4(b). Both fluxes are normalized by

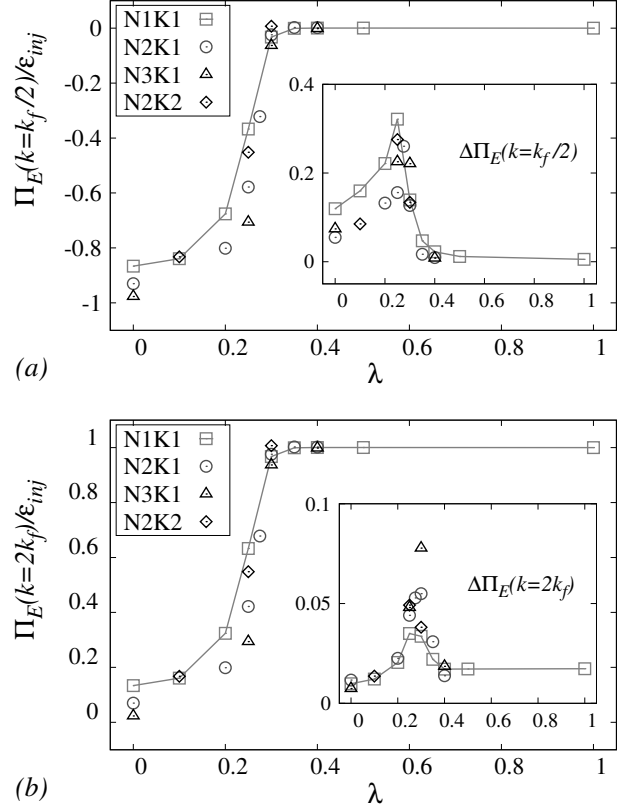


FIG. 4: Normalized energy flux at a scale larger (top) and smaller (bottom) than the forcing range *vs* λ . Insets show the fluctuations around the mean values. We plotted the guiding curve through data points from N1K1 for which we have more sample points.

the total injection rate ε_{inj} . The different symbols correspond to the different cases described in table I and correspond to an increase of Re keeping k_f fixed (runs N1K1 \rightarrow N2K1 \rightarrow N3K1) or to an increase of k_f keeping Re approximately fixed (runs N1K1 \rightarrow N2K2). For run N1K1 the transition from forward to inverse cascade is smooth, displaying a bidirectional cascade for values of λ in the range $0 < \lambda < \lambda_c \simeq 0.3$ while a pure forward cascade ($|\Pi(k_f/2)|/\varepsilon_{inj} = 0$ and $\Pi(2k_f)/\varepsilon_{inj} = 1$) is observed for values $\lambda > \lambda_c$. When Re and k_f are increased the amplitude of the inverse cascade for the points in the range $0 < \lambda < \lambda_c$ is increasing approaching the value $|\Pi(k_f/2)|/\varepsilon_{inj} = 1$ while the forward cascade is decreasing approaching the value $\Pi(2k_f)/\varepsilon_{inj} = 0$. The latter finding, suggests that at infinite Re and k_f the cascade is unidirectional and inverse for $\lambda < \lambda_c$ while it is unidirectional and forward for $\lambda > \lambda_c$. The transition is thus discontinuous. This is at difference from what observed in quasi-2D systems where the transition occurs in a continuous manner (by a bidirectional cascade) similar to a second order phase transitions, and at difference from what observed in [24] where the transition occurred

at a singular value of their model-parameter $\alpha \sim 1$.

This abrupt transition can be justified by realizing that in a bidirectional cascade the two inertial ranges ($k_\mu \ll k \ll k_f$ and $k_f \ll k \ll k_\nu$) must have different physical properties to sustain different directions of cascade. This is possible when, a new dimensional length scale ℓ_* is introduced (e.g. ℓ_* is the layer thickness in thin layer turbulence, or the Zeeman scale in rotating flows) that determines the properties of the flow due to the external mechanism. The amplitude of the inverse/forward cascade then depends on the ‘distance’ of the forcing scale ℓ_f from the critical length-scale ℓ_* . In our case, no particular scale ℓ_* is introduced by the parameter λ . On the contrary, the inertial ranges are scale invariant for all values of λ . Thus, both ranges, $\ell > \ell_f$ or $\ell < \ell_f$ effectively share the same properties and have to develop either a forward or a backward cascade, because the flow can not distinguish the large from the small scales.

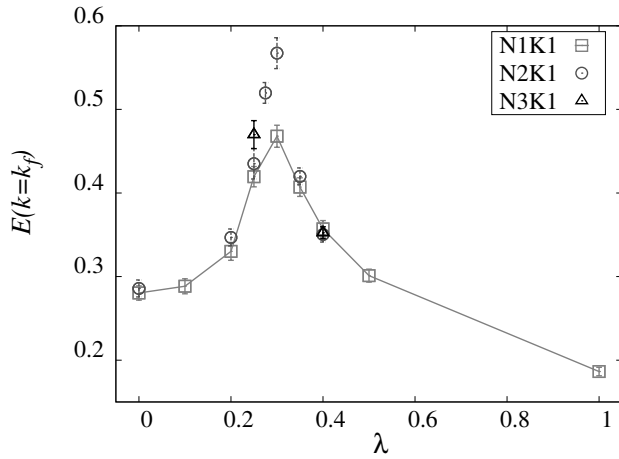


FIG. 5: Total energy content at a wavenumber inside the forcing range ($k = 11$) vs λ . We plotted the guiding curve through data points from N1K1 for which we have more sample points.

Not surprisingly the system displays interesting behavior close to the critical value λ_c . In Fig. 5 we plot, $E(k_f)$, the intensity of the spectrum at the forcing wavenumbers vs λ and for different Reynolds numbers. The response of the system is critical, showing a tendency for $E(k_f)$ to diverge as $\lambda \rightarrow \lambda_c$. This divergence is also reflected in the amplitude of the flux fluctuations $\Delta\Pi$ shown in the inset of figures 4 (where $\Delta\Pi$ of run N2K2 is multiplied by $2^{3/2}$ to account for the 2^3 more interactions involved). The existence of multiple phases for the physics of the energy containing eddies is an important remark that finds support also in recent experimental empirical findings where turbulent realizations with multiple states have been observed in swirling and in Taylor-Couette flows [27, 28].

The direction of the energy transfer can be also studied by looking at the behavior of the structure functions $S_n(r) = \langle (\delta \mathbf{u}_{\parallel}(r))^n \rangle$ where $\delta \mathbf{u}_{\parallel}(r) = (\mathbf{u}(\mathbf{x} + \mathbf{r}) - \mathbf{u}(\mathbf{x})) \cdot \mathbf{r}/r$, that have the great advantage that can be also be

easily measured in experiments. In particular, for the original NSE, the von Karman-Howarth equation states that the third order structure function is related to the direction of the cascade and it is negative for a forward transfer and positive for a backward transfer. In the form of the NSE investigated here (1) the von Karman-Howarth equation is more complicated (see, e.g. appendix A.1 of [23] for the case with $\lambda = 0$). Nevertheless, we show in Fig. 6 that even a simple measurement based on $S_3(r)$ is in good agreement with the indication that for $r > r_f = 2\pi/k_f$ the sign do change by crossing λ_c .

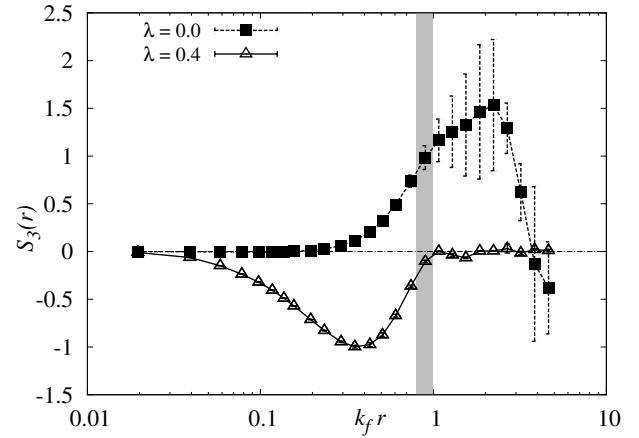


FIG. 6: Third order structure functions for two extreme cases with only direct or inverse energy cascade $\lambda = 0.4$ and $\lambda = 0$.

In this work we have demonstrated that by controlling the amplitude of the interactions in the NSE the energy cascade can change direction from forward to inverse and *vice versa*. In the model used here, this change of direction is not due to previously known mechanisms, e.g., a change in the dimensionality, a change in the ideal invariants, or the breaking of any symmetry of the original equations caused by the introduction of external forcing as in the presence of rotation or of a magnetic field, revealing that the fully non-linear dynamics of the 3D NSE is more complex than what told by the accepted phenomenology. In particular, we showed that the energy cascade is strongly sensitive to the relative dynamical weight of homochiral to heterochiral helical Fourier interactions, suggesting to search for similar footprints of inverse energy transfer also in other empirical turbulent realization. For instance, it would be interesting to check if preferential accumulation of energy in homochiral resonant triads is also observed in rotating turbulence at low Rossby numbers, in thick fluid layers, in shear flows, or in the presence of magnetic field. Our results indicate that the transition becomes discontinuous in the large Re limit. This is the first time that such a discontinuous transition is reported for the cascade direction. It is shown to be linked to the scale invariance of the system that needs to be broken for a bidirectional cascade

to exist. Most importantly it points to a new direction in which the NSE (for $\lambda = 1$) can be viewed as a system ‘close’ to criticality (for which $\lambda = \lambda_c$) that can lead to new theoretical investigations in strongly out-of-equilibrium statistical mechanics.

The research leading to these results has received funding from the European Union’s Seventh Framework Programme (FP7/2007-2013) under grant agreement No. 339032.

-
- [1] U. Frisch, *Turbulence: The Legacy of A. N. Kolmogorov* (Cambridge University Press, 1995).
 - [2] A. Brissaud, U. Frisch, J. Leorat, M. Lesieur, and A. Mazure, *Physics of Fluids* (1958-1988) **16**, 1366 (1973).
 - [3] Q. Chen, S. Chen, and G. L. Eyink, *Physics of Fluids* **15**, 361 (2003).
 - [4] L. M. Smith and F. Waleffe, *Physics of Fluids* **11**, 1608 (1999).
 - [5] A. Celani, S. Musacchio, and D. Vincenzi, *Physical Review Letters* **104**, 184506 (2010).
 - [6] A. Alexakis, *Phys. Rev. E* **84**, 056330 (2011).
 - [7] A. Pouquet and R. Marino, *Physical Review Letters* **111**, 234501 (2013).
 - [8] R. Marino, P. D. Mininni, D. Rosenberg, and A. Pouquet, *EPL (Europhysics Letters)* **102**, 44006 (2013).
 - [9] E. Deusebio, G. Boffetta, E. Lindborg, and S. Musacchio, *Phys. Rev. E* **90**, 023005 (2014).
 - [10] K. Seshasayanan, S. J. Benavides, and A. Alexakis, *Phys. Rev. E* **90**, 051003 (2014).
 - [11] K. Seshasayanan and A. Alexakis, *Phys. Rev. E* **93**, 013104 (2016).
 - [12] S. J. Benavides and A. Alexakis, *ArXiv e-prints* (2017), 1701.05162.
 - [13] L. Biferale, F. Bonaccorso, I. M. Mazzitelli, M. A. T. van Hinsberg, A. S. Lanotte, S. Musacchio, P. Perlekar, and F. Toschi, *Phys. Rev. X* **6**, 041036 (2016).
 - [14] H. Xia, D. Byrne, G. Falkovich, and M. Shats, *Nature Physics* **7**, 321 (2011).
 - [15] E. Yarom, Y. Vardi, and E. Sharon, *Physics of Fluids* **25**, 085105 (2013).
 - [16] A. Campagne, B. Gallet, F. Moisy, and P.-P. Cortet, *Physics of Fluids* **26**, 125112 (2014).
 - [17] D. Byrne and J. A. Zhang, *Geophys. Rev. Lett.* **40**, 1439 (2013).
 - [18] A. Craya, *Sci. Tech. du Ministere de l’Air* (France) (1958).
 - [19] J. Herring, D. Schertzer, M. Lesieur, G. Newman, J. Chollet, and M. Larcheveque, *Journal of Fluid Mechanics* **124**, 411 (1982).
 - [20] M. Lesieur, *Tech. Rep.*, Observatoire de Nice (1972).
 - [21] F. Waleffe, *Physics of Fluids* **4**, 350 (1992).
 - [22] L. Biferale, S. Musacchio, and F. Toschi, *Physical Review Letters* **108**, 164501 (2012).
 - [23] L. Biferale, S. Musacchio, and F. Toschi, *Journal of Fluid Mechanics* **730**, 309 (2013).
 - [24] G. Sahoo, F. Bonaccorso, and L. Biferale, *Physical Review E* **92**, 051002 (2015).
 - [25] M. Kessar, F. Plunian, R. Stepanov, and G. Balarac, *Physical Review E* **92**, 031004 (2015).
 - [26] A. Alexakis, *Journal of Fluid Mechanics* **812**, 752 (2017).
 - [27] S. G. Huisman, R. C. Van Der Veen, C. Sun, and D. Lohse, *Nature communications* **5** (2014).
 - [28] P.-P. Cortet, A. Chiffaudel, F. Daviaud, and B. Dubrulle, *Physical review letters* **105**, 214501 (2010).